

Experimental Study on Sensitivity to Temperature Stress of the Permeability of Weakly Cemented Sandstone

Z Y SONG^{1,2}, H G JI², S YOU², J TAN¹ and H WANG¹

¹Mine construction branch, china coal research institute, Beijing100013, China

²School of civil and resource engineering, University of science and technology Beijing, Beijing100083, China

szhaoyang123@126.com, jihongguang@ces.ustb.edu.cn, 64849285@qq.com, 378598485@qq.com, 787577336@qq.com

Abstract. In order to explore the meso-structural characteristics of weakly cemented sandstone and its permeability characteristics under multi-field coupling, SEM scanning electron microscopy and Top Industries rock triaxial remoter system have been used. On the basis of studying the microstructure of weakly cemented sandstone, the sensibility of its permeability to temperature and confining pressure is preliminarily study. The results show that the compaction effect of weakly cemented sandstone is poor, and the elastic particles are compacted and degenerated. It features concave-convex contact, and base cementation playing a main role. Because of the difference in pore structure, within the experimental range, when the temperature rises and the confining pressure increases, the influence of confining pressure on the mineral particles leads to the change of permeability. The confining pressure increases the plastic deformation of the intergranular particles. There is an irreversible phenomenon in the process of rising and falling of the confining pressure, while the effect of temperature on permeability is small. The three coupling surfaces of permeability, temperature and confining pressure of weakly cemented sandstone with different granularities are developed, and the corresponding coupling equations are presented. Therefore, during construction in the weakly cemented stratum, substantial deformation of surrounding rock due to sensitivity of permeability to confining pressure should be avoided, and active support measures should be strengthened in the aquifer layer.

1. Introduction

Weakly-cemented stratum is a special kind of sedimentary sandstone widely distributed in the Jurassic and Cretaceous strata in the mining area of western China. The stratum mainly consists of weakly cemented sandstone with low constituent maturity and structure maturity. It is rich in rigid particles and features low mechanical strength due to poor cementation and compaction. With exposure to water, the phenomenon of disintegration after argillization is serious, thus causing higher requirements for the stability support of the surrounding rock during underground engineering in western China^[1]. Due to the existence of groundwater, the seepage, temperature, and pressure of weakly cemented sandstone would interact with each other. The osmotic pressure and temperature will affect the stress distribution of the surrounding rock. Especially, the high temperature and pressure conditions in deep underground would result in even greater influences towards the permeability in the strata. Meanwhile, the stress redistribution will inevitably lead to the change of the internal permeability of rock mass.

At present, researchers have analyzed and studied three coupling interactions of rock mass through mathematical models, numerical simulation and related experimental studies, which has yielded certain



research results. WANG Xiaojiang and his colleagues^[2] used a triaxial coupling testing machine to carry out the seepage test of deformation and failure process of coarse sandstone under different confining pressures. The variation of permeability during the deformation and failure process of coarse sandstone as well as the influence of confining pressure on its permeability were analyzed. HUANG Xianwu and his colleagues^[3] conducted steady-state infiltration experiments on the fractured sandstone, which proved the relations among permeability, the non-Darcy beta factor and the porosity. Through the experimental study, HE Yulong^[1] explored the highly nonlinear complex coupling effect among the temperature field, seepage field, and deformation field. LI Shiping and his colleagues^[4-5] conducted the experimental study of permeability changing pattern during the sandstone stress-strain process, and presented the permeability-strain equation of the sandstone. ZHANG Shouliang and other researchers^[6] tested the variation law of permeability during the whole process of stress-strain of sandstone with different cementation degree by using high-temperature and high-pressure rock triaxial apparatus, and thus analyzing the relationship between rock permeability and its stress state and mechanical parameters. KANG Han^[7] carried out triaxial tests on sandstone of medium and fine grain size in Sichuan Province to analyze the strength and deformation characteristics of sandstone of different grain sizes. He also explored the effect of grain size on the strength of sandstone. ZHOU Hang and his colleagues^[8] conducted experiments on the mechanics and permeability of sandstone with different granularities, and obtained the pattern and characteristics of the correspondence between the variation of permeability and the deformation features. WANG Huailing and others^[9] conducted the infiltration test of the whole stress-strain process of limestone and sandstone through the servo testing machine, which gave insight to the relationship between axial stress and permeability of rock during deformation and failure, as well as the influence of circumferential deformation on permeability. The variation law of osmotic pressure difference with time before and after destruction of rock sample has also been analyzed. WANG Wei and his colleagues^[10] conducted a triaxial seepage-stress coupling test while factoring into the effect of seepage hydraulic pressure on low-permeability granite. The stress-strain relationship of the rock features typical brittle characteristics. The study resulted in the equation between permeability and volumetric strain. Such main research work focuses on the change of permeability in the process of total stress and strain. However, the sensitivity of permeability under triaxial compression with different temperature conditions is a relatively less studied area.

In this paper, the weakly cemented sandstone in Ordos Hongqing River mining area is studied through SEM scanning electron microscopy, with analysis of the meso-structure of weakly cemented sandstone. The contact features between the skeleton and the particle are also described. On the basis of the study of the meso-structure, it preliminarily explored the sensitivity characteristics of permeability of weakly cemented sandstone to temperature and confining pressure, and reveals the three coupling equations of permeability, temperature, and confining pressure of weakly cemented sandstone.

2. Meso-structure experiment and analysis of weakly cemented sandstone

The weakly cemented sandstone samples were all taken from the underground of 680m depth in the Hongqing River mining area in Ordos. The stratum of the rock sample was the Mesozoic Jurassic system Middle Zhiluo group. The stratum featured monoclinic structure, with the dip angle of 1-3°. The lithology of this stratum was gray-green siltstone, while the fine-grained and medium-grained sandstone featured inter-layer output, and the sandstone contained carbon bits and coal stripe band. The maximum principal stress in the sampling interval was 20.5-22.5MPa. The minimum horizontal principal stress was 17.5-19MPa, and the vertical stress was 13-15.5MPa. The meso-structure characteristics of typical weakly cemented sandstone have been studied through scanning electron microscope. In the experiment, SEM scanning electron microscopy was used with a resolution of 3.0nm at high vacuum. High-speed observation of the surface morphology of solid samples was performed through electron microscopy with a highly sensitive secondary electron probe and a backscatter electron probe. The sample was dried (it's important not to polish randomly), and then placed into the coating machine to go through gold spray process. After that, through the conductive adhesive, it was fixed on the stage, and finally put into the chassis for vacuumizing before photo acquisition. The test results is illustrated in Figure 1.

According to the different characteristics of the weakly cemented sandstone samples under SEM, and with the different mesostructural types, the cementation patterns, particle size and morphology, particle contact modes, pore features, and other meso-structure features of the samples have been mainly observed [11]. As can be seen from Figure 1, the weakly cemented sandstone is composed of rigid particles as the basic skeleton, forming a skeleton-like structure. The structure is porous, loose and evenly distributed, and the fine clay particles are arranged unevenly and randomly. Adhesion sticky particles are attached to the surface of the particles, mainly in the form of film or at the contact point between the particles, playing the role of cementation for different particles. The grains of weakly cemented sandstone are randomly arranged and lack a consistent orientation of the structural units. The arrangement and contact of particles are mainly dominated by agglomeration.

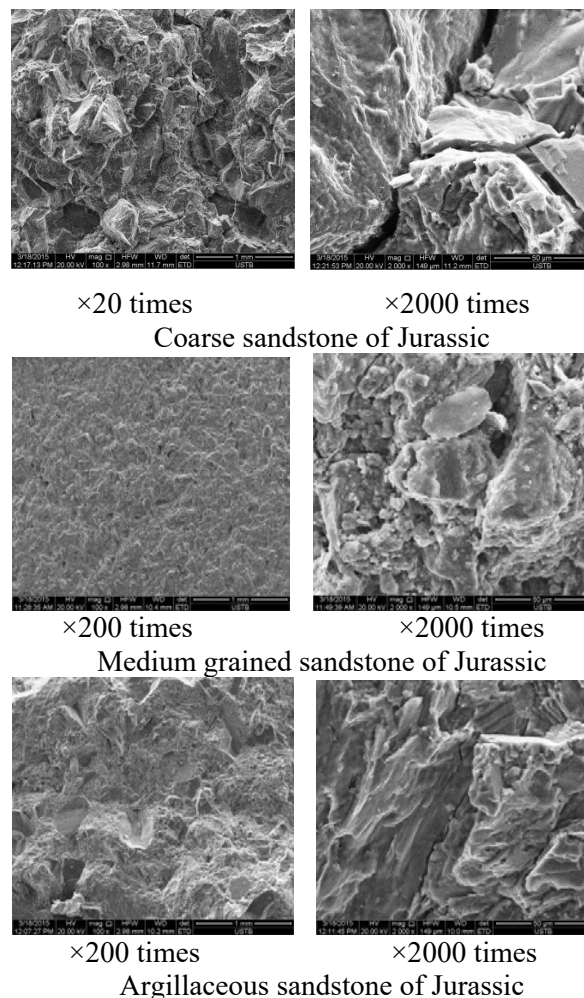


Figure 1. Electron microscopy of weakly cemented sandstone samples

In figure 1. (a) the pore space of the Jurassic coarse sandstone structure consists of open and evenly distributed particles and intergranular pores. The intergranular cementing method is pore cementing and contact cementing, with poor particle roundness. The particles feature surface contact and concave-convex contact, with loose meso-structure [12-13]. High porosity causes easy entry of water into the sandstone, resulting in the argillization of cementation materials, as well as the swelling of the particulate matter itself which causes swelling of the meso-structure upon contact with water. In figure 1 (b) the medium-grained sandstone of Jurassic is relatively uniform in distribution. Compared with the Jurassic coarse sandstone, the Jurassic medium-grained sandstone has a higher degree of cementation, featuring base cementation and a large amount of interstitial material. Clastic particles are scattered and detached with

each other. The clay mineral is mainly illite, which exerts important influences on the cementation between the particles. When the particle size distribution is good and the performance of the particle cementation material is good, the grains of the weakly cemented sandstone are fully exposed during the stress loading. Most of the particles would contribute to the particle contact force of the model due to better particle size distribution, resulting in a higher peak intensity than the coarse sandstone. In figure 1 (c) the argillaceous sandstone of Jurassic has a compact structure featuring base cementing with no obvious grain boundaries. It also shows clear rock fragments and sharp edges, with typical features of brittle failure of rock samples. Weakly cemented sandstone meso-structural characteristics are presented in Table 1 as follows.

3. Weakly cemented sandstone seepage test and test plan

Weakly cemented sandstone seepage test has been performed on Top Industries rock triaxial rheometer in the Northeastern University. The system is equipped with three sets of independent control system: axial pressure, confining pressure, and pore water pressure. It can perform Rock Permeability Test under Field Action of stress field, temperature field, and chemical field. Axial maximum load is 600KN, the maximum confining pressure 60MPa, the maximum water pressure 60MPa, and the maximum temperature 90 °C. The linear displacement sensor LVDT has been used to measure the axial displacement accurately. The hoop strain is measured through a ring strain gauge fixed in the middle of the sample. The system provides stress control and displacement control, along with types of pore water injection, namely controlling the flow and the pressure. The confining pressure loading rate is 0.2Mpa/s. Rock specimen physical parameters can be found in Table 2. The samples used in the experiment have been dried at low temperature for 48h and cooled in a desiccator. 2 sets of experiments have been conducted by using the same batch of rock samples. During each measuring point in the acquisition of test data, constant pressure and flow method have been used to collect data. Test equipment and test specimen installation diagram are shown in Figure 2.

Table 1. Description of the fine characteristics of weakly cemented sandstone

Rock samples	Particles Morphology	Pore characteristics	Microfissure	Breakage characteristics
Argillaceous sandstone of Jurassic	particle boundaries not obvious	Not obvious	Little	Layered structure, serrated section
Medium grained sandstone of Jurassic	moderately obvious boundaries, interstitial viscous particles	Obvious pores between particles	Fissures in the boundaries of particles, partial development of foliation structure	Layered structure with traces of small particles stripping
Coarse sandstone of Jurassic	Obvious grain boundaries, interstitial viscous particles	Moderately obvious pores between particles	Relatively bigger fissures in the boundaries of particles, partial development of foliation structure	Traces of small particles stripping along the grain boundaries



Figure 2. Test instrument schematic diagram

Specific test methods are as follows: The first set of experiment concerns the weakly cemented sandstone temperature sensitivity test. Researchers set the confining pressure respectively as 5MPa, 7.5MPa, 10MPa, 12.5MPa, and 15MP. After it was made stable, the pore water pressure was risen to 1MPa and kept constant. Then the temperature was gradually increased from 20°C (room temperature) to 30 °C, 40 °C, 50 °C, 60 °C, 70 °C, and 80 °C. The permeability of rock samples at each temperature level was measured to study the permeability of different grain sizes of weakly cemented sandstone. (Metal mine rock temperature over 700m deep in our country generally exceeds 35 °C); In the second group of experiments, the stress sensitivity of weakly cemented sandstone was tested. After the temperature was set at 20 °C, 30 °C, 40 °C, 50 °C, 60 °C, 70 °C and 80 °C respectively, the pore water pressure was increased to 1MPa and remained at that level. The confining pressure was then gradually increased to 5MPa, 7.5MPa, 10MPa, 12.5MPa and 15MPa. the permeability under each confining pressure point was measured to study the pressure sensitivity under different confining pressures.

Before the test, the sample was evacuated and filled with distilled water for 48h to ensure that the seepage flow in the sample was one-way during the test. The experiment used distilled water as seepage medium, which was a kind of incompressible fluid. The initial pore distribution of rock mass was homogeneous with no obvious fracture. Darcy's steady flow method was used to test the permeability of the rock samples. The permeability was calculated according to the flow rate of rock cross-section per unit time and the osmotic pressure difference between two ends of rock samples^[14, 15]. According to Darcy's law, the formula is:

$$k = \mu \frac{v}{A\Delta t} \frac{L}{p_{in} - p_{out}} \quad (1)$$

In the formula, k stands for the permeability of rock sample (mD), μ is the dynamic viscosity coefficient of water (Pa · s), the values of different temperatures are accessible through the table, and V is the seepage fluid out of the moment (cm³); L is the length of the rock specimen (cm); A is the cross-sectional area of the rock specimen (cm²); Δt for time (s); P_{in} is the pressure at the bottom of the rock specimen (Pa); and P_{out} is the pressure at the top of the rock specimen.

Tab.2 The physical parameters of the sample

Rock samples	diame- ter/mm	height /mm	volume /cm ³	Mass g	density/ (g/cm ³)	wave velocity / (m/s)	porosity /%
Jurassic coarse sandstone	49.7	99.8	193.61	375.72	1.94	1644.80	20.58~22.05
Medium grained sandstone of Juras- sic	49.64	99.9	193.34	465.27	2.41	2549.77	12.76~14.98
Argillaceous sand- stone of Jurassic	49.85	99.97	195.11	402.46	2.06	2129.07	7.21~10.03

4. Results and analysis

4.1 Influence of temperature on the permeability of weakly cemented sandstone

With room temperature of 20 °C, confining pressure of rock sample 5MPa, and pore pressure 1MPa, the permeability values of sandstone with different grain sizes serve as the base values, and the permeability change rate of each sample relative to the reference point is defined as the absolute rate of decrease of the permeability (Δk). The rate of change of the permeability of the latter temperature point relative to the previous temperature point is defined as the relative rate of decrease of the permeability of the rock sample (Δv)::

$$\Delta k = \frac{(k_0 - k_{ii})}{k_0} \times 100 \quad (2)$$

$$\Delta v = \frac{(k_{ii-1} - k_{ii})}{k_{ii-1}} \times 100 \quad (3)$$

In the formula: k_0 is the permeability with the confining pressure of 5MPa, pore pressure 1MPa, and the temperature measured 20 °C. k_{ii} stands for permeability at any temperature and pressure measurement point.

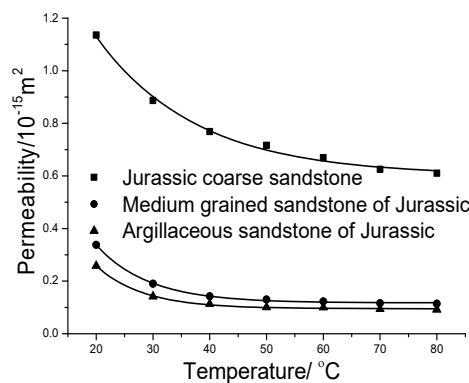


Figure 3. Test instrument schematic diagram the permeability of different grain size sandstone varies with the temperature curve when the confining pressure is 5MPa

After the confining pressure was set to be constant at 5 MPa, the pore water pressure was increased to 1 MPa and kept constant. The temperature was gradually raised from 20 °C (room temperature) to 30 °C, 40 °C, 50 °C, 60 °C, 70 °C, and 80 °C. The permeability of rock samples at each temperature was measured to obtain the curve of the rate of decrease of permeability of sandstone with different grain sizes and temperatures, as shown in Figure 3.

Increasing the temperature would result in a significant decrease in porosity and a decrease in permeability with increasing temperature. The increase of temperature leads to the decrease of permeability due to the volume expansion of mineral particles. Also, the increase of temperature leads to the decrease of viscosity of water and the increase of permeability [16-19]. From the results of the test of absolute decrease rate and relative decrease rate at different temperatures of sandstone with different grain sizes in Figure 4, the decrease of permeability caused by the volume expansion of mineral particles is dominated by the increase of temperature within the experimental range. The porosity of the same cemented sandstone also differs in the condition of same confining pressure but different temperatures, and in the condition of same temperature but different confining pressures. At each measured temperature, the overall trend in porosity appears to decrease exponentially with increasing temperature. The permeability of sandstone, fine-grained sandstone and medium-grained sandstone with different grain sizes is lower than that of coarse-grained sandstone.

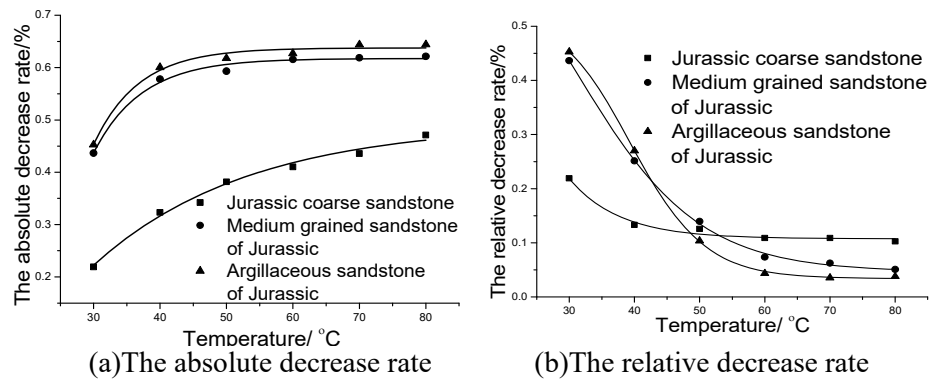


Figure 4. The absolute decrease rate and relative decrease rate of sandstone at different particle size

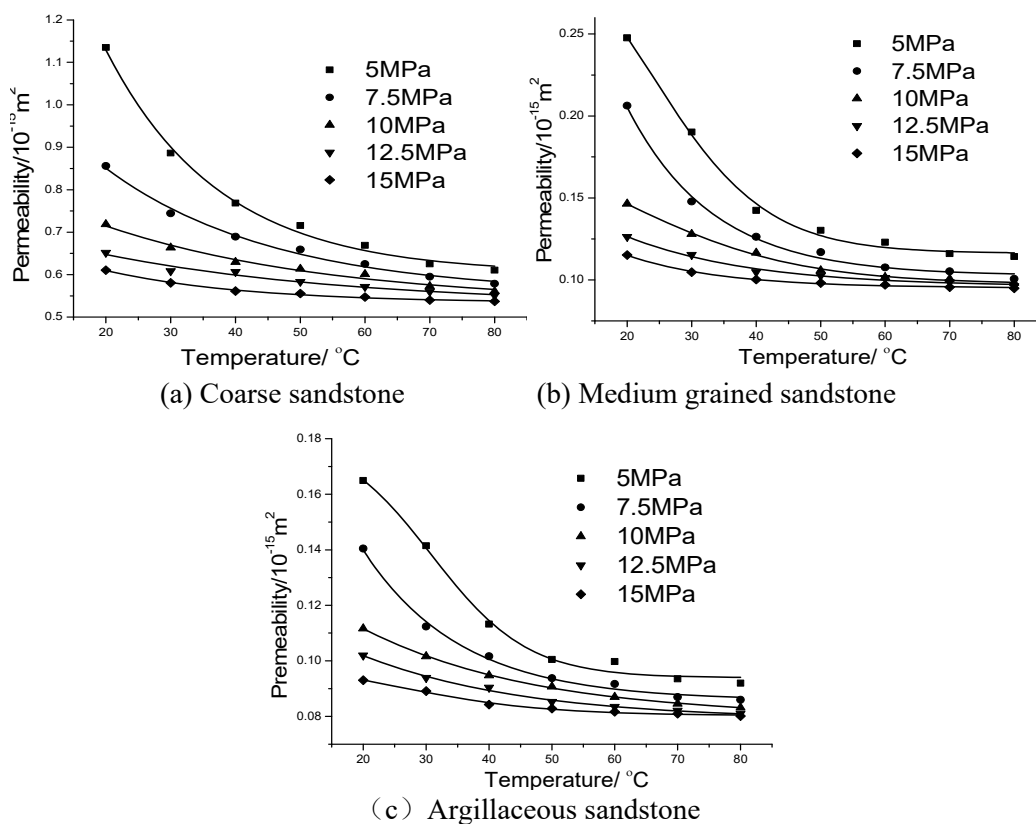


Figure 5. Temperature sensitivity of core permeability under different confining pressure

According to the temperature sensitivity test of core permeability under different confining pressures illustrated in Figure 5, when the measuring conditions are changed from 5MPa and 20 °C to 5MPa and 30 °C, the absolute rate of decrease of coarse sandstone permeability decreases to 21.9%. When the measuring condition is 5MPa and 40°C, the absolute decrease rate of permeability reaches 32.3%. When it is 5MPa and 80°C, the absolute decrease rate reaches as high as 47.1%. For the medium grained sandstone, when the measuring condition is changed from 5MPa、20°C to 5MPa and 30°C, the absolute decrease rate of permeability reaches 57.8%. It stands at 61.8% with 5 MPa and 40 °C, and 62.16% with 5MPa and 80°C. In terms of the fine grained sandstone, the absolute decrease rate of permeability is similar to that of medium grained sandstone. The comparison shows variation porosity of the medium and fine grained sandstones are more affected by the temperature than that of the coarse sandstone.

4.2 Influence of loading and unloading of confining pressure on permeability

In the Stress Sensitivity Test of Weakly Cemented Sandstone, after the confining pressure was increased to 5MPa and kept constant, the pore water pressure was increased to 1MPa and kept constant. The confining pressure was then gradually increased to 7.5MPa, 10MPa, 12.5MPa, 15MPa, 17.5MPa, and 20MPa. Permeability under each confining pressure point was measured to study the pressure sensitivity of permeability of sandstone with various particle sizes under different confining pressures.

As the confining pressure increased, both the rock lateral strain and longitudinal strain increased, as shown by the permeability curve of coarse sandstone during the process of confining pressure loading and unloading presented in Figure 6. Weakly cemented sandstone particle size, grading and cement content exerted significant impact on permeability. Coarse sandstone contained bigger particles, and its cementation material (whose biggest ingredient is chlorite) had a relatively better framework structure. The porosity was also the largest. Under the same conditions, the influence of confining pressure on permeability was most obvious. Increasing confining pressure would result in a significant decrease in porosity, and permeability decreasing along with increasing confining pressure. During the pressure relief process, the permeability rose slightly, but not restored to the initial permeability under the original pressure. During the loading-unloading process, the transverse strain and the longitudinal strain are plastically deformed, and the pore irreversibly deformed, resulting in the decrease of the permeability.

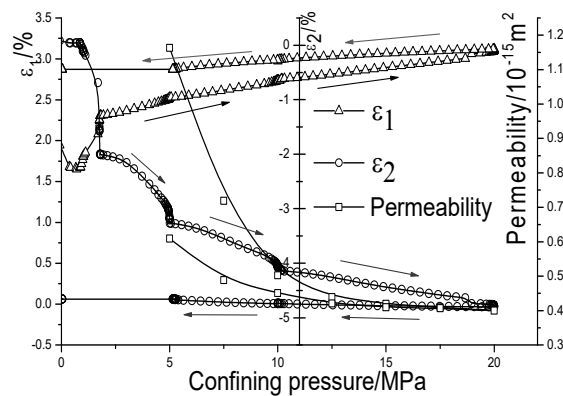


Figure 6. The permeability curve of coarse sandstone in the process of confining pressure and unloading

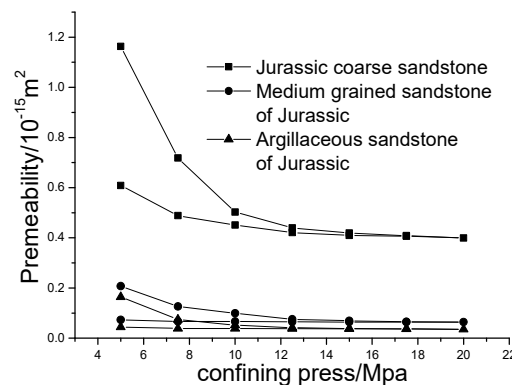


Figure 7. The permeability of sandstones with different particle sizes in loading and unloading path of confining pressure

Figure 7 shows the permeability under different loading and unloading paths with sandstone of different grain sizes, while Figure 8 presents the absolute decrease rates and relative decrease rates of loading and unloading paths with sandstone of different grain sizes. The analysis shows that the same rock features different porosities in both the condition of the same confining pressure but different temperature, and the condition of the same temperature but different confining pressure. Under the measured confining pressure, permeability sensitivity to confining pressure of fine-grained sandstone and me-

dium-grained sandstone, with lower porosity, is lower than that of coarse sandstone. When the measurement conditions were changed from 5MPa to 10MPa, the absolute decrease rate of permeability of coarse sandstone reached 38.2%, and changed to 63.9% when it became 15MPa. The absolute decrease rate of permeability was as high as 65.6% for 20MPa. For the medium-grained sandstone, the absolute decrease rate of permeability reached 52.08% when the condition changed from 5MPa to 10MPa. The rate stood at 63.6% when it became 15MPa, and 68.6% when it was 20MPa. In terms of the fine-grained sandstone, when the measuring conditions were changed from 5MPa to 10MPa, the absolute decrease rate reached 68.2%. When it became 15MPa, the absolute decrease rate of permeability registered at 76.3%. For 20MPa, the absolute decrease rate of permeability was 78.6%. The comparison shows that the influence of the change of surrounding rock on the permeability of coarse-grained sandstone, medium-grained sandstone and fine-grained sandstone gradually increases.

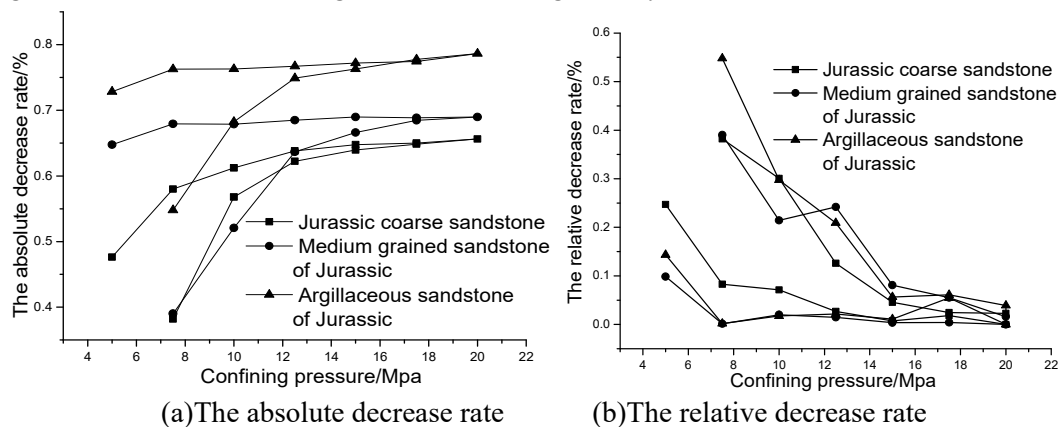


Figure 8. The absolute decrease rate and relative decrease rate in the loading and unloading path of sandstones of different grain sizes

4.3 Temperature-pressure-permeability coupling and curved surface equation

Coupling of temperature and confining pressure is a typical environment for the mechanics of deep rock mass. The grain structure, cementation strength, defects and fissures randomly distributed in the weakly cemented sandstone under the coupling of temperature and confining pressure are the main causes of the rock damage. The damage of the meso-structure of the weakly cemented sandstone under high temperature and external load is the direct result of changes in rock permeability. There is bound to be a certain functional relation among the permeability characteristics, the temperature, and the stress fields, specifically:

$$K=f(T, \sigma) \quad (4)$$

Table 3. Fitting constant of the permeability, temperature and confining pressure coupling of weakly cemented sandstone with different particle sizes

Rock	Fitting constant							R2
	z0	A	xc	w1	yc	w2	theta	
Coarse sandstone of Jurassic	12096.4	-12095.9	27.1	31969.5	19.9	1818.9	-0.18	0.92
Medium grained sandstone of Jurassic	1558.9	-1558.82	53.87	1222.98	14.4	8954.86	1.38	0.92
Medium grained sandstone of Jurassic	1767.2	-1767.1	53.74	13948.8	15.11	1825.38	-0.19	0.93

Directly through the seepage-temperature-confinement coupling laboratory experiments, this paper presents the curved surface fitting between the different sizes of weakly cemented sandstone permeability and temperature, and confining pressure, as shown in Figure 9. According to the curved surface morphology of temperature-confining pressure coupling surface of sandstone with different sizes, as

presented in Figure 9, the nonlinear curve fitting of the test data shows that the permeability-temperature-confinement coupling relationship of weakly cemented sandstone samples with different sizes can be addressed by the Gaussian curved surface equation to conduct fitting.

The surface fitting equation is:

$$z = z_0 + A \exp\left(-\frac{1}{2} \left(\frac{x \cos(\theta) + y \sin(\theta) - x_c \cos(\theta) - y_c \sin(\theta)}{w_1} \right)^2 - \frac{1}{2} \left(\frac{-x \sin(\theta) + y \cos(\theta) + x_c \sin(\theta) - y_c \cos(\theta)}{w_2} \right)^2 \right) \quad (5)$$

In the formula, z_0 , A , x_c , w_1 , y_c , w_2 , and θ are all fitting constants. Changes of the constants are related to particle size distribution, particle contact mode and cementation status of weakly cemented sandstone.

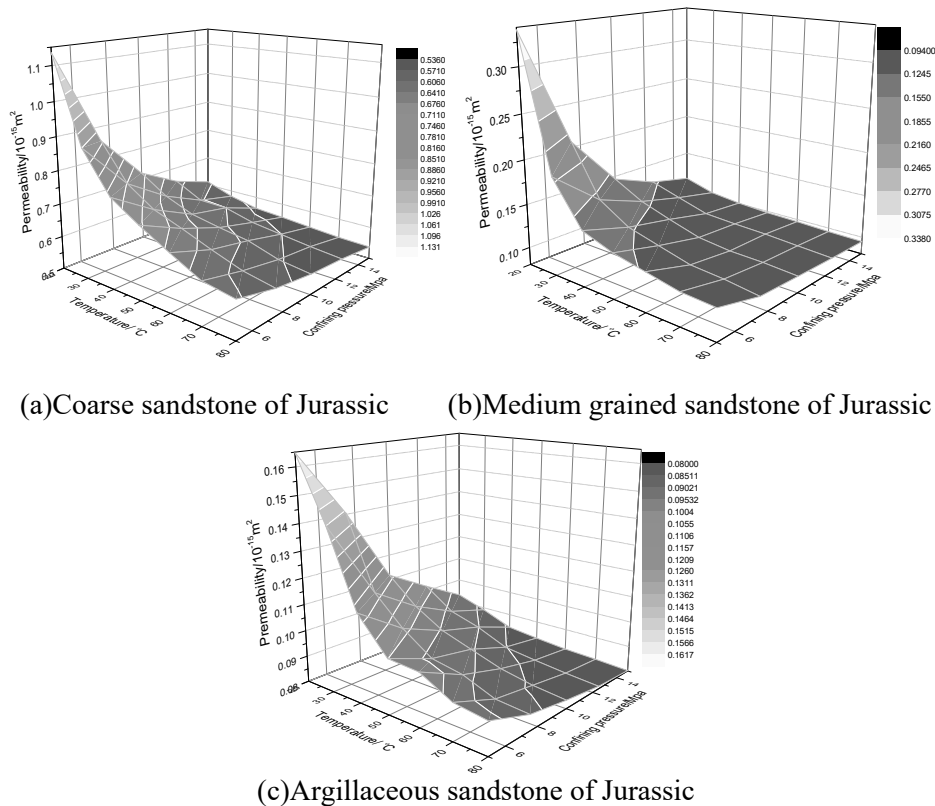


Figure 9. Permeability - temperature - confining pressure coupling surface of sandstones with different particle sizes

5. Conclusion

Jurassic coarse sandstone and Jurassic medium grained sandstone feature poor compaction effect, deformation of detrital grains after compaction, directional orientation of grains, and concave-convex contact. It is characterized by base cementation with large intergranular spacing, and the porosity filling clay minerals occupy effective pore space. Cementitious materials are mainly clay-based cementation. Jurassic argillaceous sandstone is dominated by clay cementation and alteration, with better compaction effect.

The decrease of permeability caused by the volume expansion of mineral particles dominates when the temperature rises and the confining pressure increases within the experimental range. The absolute decrease rate of permeability of argillaceous sandstone is similar to that of medium grained sandstone. The changes of porosity affected by temperature and confining pressure is more pronounced compared to that of coarse sandstone.

The plastic deformation of rock samples appears when the confining pressure increases. There is irreversible phenomenon of the permeability during the rising and falling with the confining pressure. The decrease rate of permeability of coarse sandstone during confining pressure changes is smaller than that of fine grained sandstone. The smaller particles are, the more sensitive they are to confining pressure. From a microscopic point of view, due to the high content of clay minerals in the weakly cemented sandstone, the seepage channel between the particles can be easily blocked. Therefore, the permeability of the weakly cemented sandstone, which constitutes the weakly cemented stratum, is much lower than that of ordinary sandstone.

Through the study on the change of internal structural characteristics and permeability rate of sandstone under the influence of the temperature and confining pressure of weakly cemented sandstone, the permeability-temperature-confining pressure coupling surface of weakly cemented sandstone with different granularities are drawn and presented, along with the corresponding coupling equations, thus providing a theoretical basis for the quantitative study of the permeability of weakly cemented sandstone.

References

- [1] HE Yulong, YANG Zhongli. Testing study on variational characteristics of rockmass permeability under loading-unloading of confining pressure[J]. Chinese Journal of Rock Mechanics and Engineering, 2004, 23 (3): 415-419.
- [2] WANG Xiaojiang, RONG Guan, ZHOU Chuangbing. Permeability experimental study of gritstone in deformation and failure processes[J]. Chinese Journal of Rock Mechanics and Engineering, 2012, 31 (s1): 2940-2947.
- [3] Huang Xanwu, TANG Ping, MIU Xiexing et al. Testing study on seepage properties of broken sandstone[J]. Rock and Soil Mechanics, 2005, 26(9): 1385-1388.
- [4] LI Shiping, LI Yushou, WU Zhenye. The permeability strain equations relating to complete stress-strain path of the rock[J]. Chinese Journal of Geotechnical Engineering, 1995, 17(2): 13-19.
- [5] Li S. P., Wu D. X., Xie W. H. et al. Effect of confining pressure, pore pressure and specimen dimension on permeability of Yinzhuang sandstone[J]. Int. J. Rock Mech. & Min. Sci., 1997, 34(3-4): 435-441.
- [6] ZHANG Shouliang, SHEN Chen, DENG Jingen. Testing study on the law of permeability variation in process of rock deformation and damage[J]. Chinese Journal of Rock Mechanics and Engineering, 2000 (s1): 885-888.
- [7] KANG Hang. Experimental Study on Mechanical characteristics of triaxial compression of sandstone in different size[J]. Subgrade Engineering, 2013, (6) :94-96.
- [8] ZOU Hang, LIU Jiangfeng, BIAN Yu, et al. Experimental study on mechanics and permeability characteristics of different granularities of sandstone [J]. Chinese Journal of Geotechnical Engineering, 2015, 37 (08): 1462-1468.
- [9] WANG Huanling, XU Weiya, YANG Shengqi. Experimental investigation on permeability evolution law during course of deformation and failure of rock specimen[J]. Rock and Soil Mechanics, 2006, 27(10): 1703-1708.
- [10] WANG Wei, XU Yadong, WANG Rubin, et al. Permeability of dense rock under triaxial compression[J], Chinese Journal of Rock Mechanics and Engineering, 2015, 34(1): 40-47.
- [11] YU Qinglei, YANG Tianhong, ZHENG Chao, et al. Numerical analysis of influence of rock meso-structure on its deformation and strength[J]. Rock and Soil Mechanics, 2011 (11): 3468-3472.
- [12] ZHOU Cuiying, TAN Xiangshao, DENG Yimei, et al. Research on softening micro-mechanism of special soft rocks[J]. Chinese Journal of Rock Mechanics and Engineering, 2005, 24(3): 394-400.
- [13] SHI Xian, CHENG Yuanfang, JIANG Shu, et al. Experimental study of microstructure and rock properties of shale sample[J]. Chinese Journal of Rock Mechanics and Engineering, 2014, 33(s2): 3439-3445.
- [14] LIANG Bing, GAO Hongmei, LAN Yongwei. Theoretical analysis and experimental study of relation between rock permeability and temperature[J]. Chinese Journal of Rock Mechanics and Engineering, 2005, 24(12): 2009 - 2012.

- [15] HUANG Yuanzhi, WANG Enzhi. Experimental study on coefficient of sensitiveness between percolation rate and effective pressure for low permeability rock[J].Chinese Journal of Rock Mechanics and Engineering,2007,26(2):410-414.
- [16] SUN Dongsheng,LI Awei,WANG Hongcai,et al.Experiment on anisotropy of permeability with tight sandstone[J].Progress in Geophys,2012,27(3):1101-1106.
- [17] LI Hongyan,QI Qingxin,LIANG Bing. Research on coal permeability evolution laws and multi-scale effect[J]. Chinese Journal of Rock Mechanics and Engineering,2010,29(6):1192-1197..
- [18] METWALLY Y M,SONDERGEID C H.Measuring low permeability of gas-sands and shales using a pressure transmission technique[J].International Journal of Rock Mechanics and Mining Sciences,2011,48(7):1135-1144.
- [19] YANG Xinle,ZHANG Yongli,LI Chengquan,et al.Experimental study of desorption and seepage rules of coal-bed gas considering temperature conditions[J].Chinese Journal of Geotechnical Engineering,2008,30(12):1811-1814.